

## Composites Containing Fullerenes and Polysaccharides: Green and Facile Synthesis, Biocompatibility, and Antimicrobial Activity

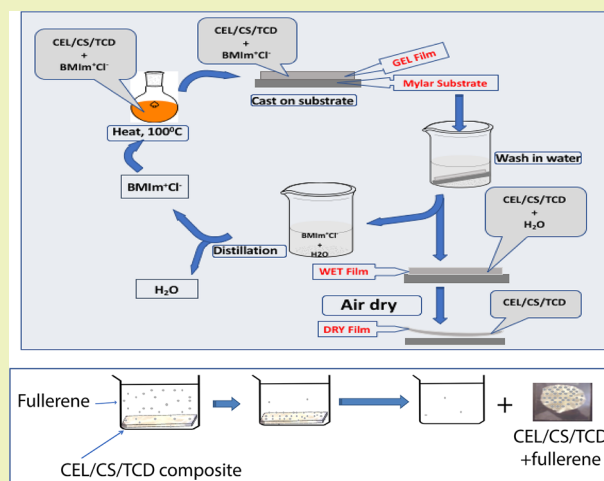
Simon Duri, April L. Harkins, Anna J. Frazier, and Chieu D. Tran\*

Department of Chemistry, Marquette University, 535 N. 14th Street, Milwaukee, Wisconsin 53233, United States

## Supporting Information

**ABSTRACT:** By use of a green and simple ionic liquid, butylmethylimidazolium chloride ( $\text{BMIm}^+\text{Cl}^-$ ) as a sole solvent, we developed a novel, green, and simple method to synthesize biocompatible composites containing polysaccharides (cellulose (CEL), chitosan (CS), and  $\gamma$ -cyclodextrin ( $\gamma$ -TCD)) and fullerene derivatives (amino- $\text{C}_{60}$  and hydroxy- $\text{C}_{60}$ ). The composites obtained (100%CEL, 100%CS, [CEL+ $\gamma$ -TCD] and [CS+ $\gamma$ -TCD]) readily adsorb amino- $\text{C}_{60}$  and hydroxy- $\text{C}_{60}$ . Kinetics and adsorption isotherm results indicate that the fullerene derivatives physically adsorbed onto the surface of the CEL-based composites and subsequently desorbed from the composites when they were soaked in water. Conversely, because both fullerene derivatives strongly adsorbed onto the surface and subsequently diffused into the pores within the matrix of the CS-based composites, it was possible to synthesize (CS+amino- $\text{C}_{60}$ ), (CS+hydroxy- $\text{C}_{60}$ ), (CS+ $\gamma$ -TCD+amino- $\text{C}_{60}$ ), and (CS+ $\gamma$ -TCD+hydroxyl- $\text{C}_{60}$ ) composites. Microbial assay results show that adding  $\gamma$ -TCD, amino- $\text{C}_{60}$ , and/or hydroxyl- $\text{C}_{60}$  to CS substantially increases the composite's ability to reduce the growth of antibiotic-resistant bacteria such as Vancomycin-resistant *Enterococcus* (VRE). Biocompatibility assays indicate that hydroxy- $\text{C}_{60}$  and amino- $\text{C}_{60}$  are not cytotoxic to humans when encapsulated into CS composites. Taken together, the (CS+ $\gamma$ -TCD+fullerene) composites are well suited for various applications ranging from dressing to treat chronically infected wounds to nonlinear optics, biosensors, and therapeutic agents.

**KEYWORDS:** Ionic liquid, Cellulose, Chitosan, Cyclodextrin, Antibiotic-resistant bacteria, Chronic infected wounds



## INTRODUCTION

Fullerenes have been the subject of wide and intense studies in many disciplines including chemistry, physics, and materials science.<sup>1–5</sup> Because of their unique structure, fullerenes have many interesting and unique properties including nonlinear effect, biological activity, optical limiting effect, and superconductivity.<sup>1–20</sup> For example,  $\text{C}_{60}$  and its derivatives have effectively served as agents and/or materials in thermoresponsive materials, sensors to detect illicit drugs (e.g., amphetamine), endocrine disruptors (e.g., bisphenol A), smart optical filters, and photodynamic therapy [i.e.,  $\text{C}_{60}$  and  $\text{C}_{70}$  are strong photosensitizers to generate singlet oxygen ( $^1\text{O}_2$ ). The efficiencies of generating  $^1\text{O}_2$  by fullerenes are 2–3 times higher than well-known photosensitizers such as rose bengal.], magnetic imaging, neuroprotection, anti-apoptosis, antioxidants, and antibacterials to inhibit growth of various bacteria and fungi such as *Propionibacterium acnes*, *Staphylococcus epidermidis*, *Candida albicans*, *Malassezia furfur*, *E. coli*, vancomycin-resistant *Enterococcus faecalis* (VRE), and of various cancer cells and HIV virus.<sup>1–20</sup> Efforts have been made, therefore, to use  $\text{C}_{60}$  to prepare novel and high performance materials that have these antimicrobial and antiproliferative

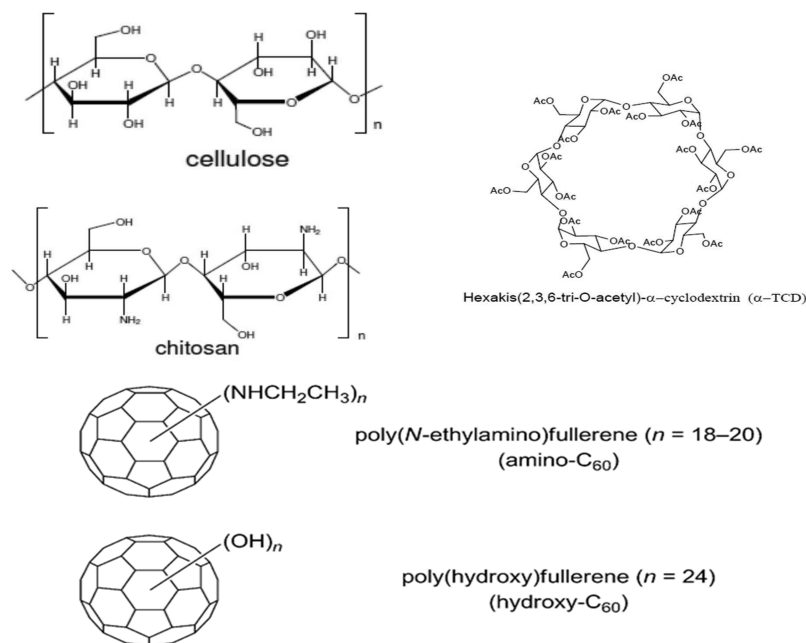
properties. Unfortunately, in spite of considerable efforts, advances in this field are rather limited. This may be due to the fact that  $\text{C}_{60}$  has relatively poor solubility, miscibility, and processability. As a consequence, to date,  $\text{C}_{60}$ -based materials were made by covalently binding or grafting  $\text{C}_{60}$  onto manmade polymers.<sup>21–30</sup> The rather complicated, costly, and multistep process is not desirable as it requires not only expertise in synthesis but also may inadvertently alter properties of  $\text{C}_{60}$ , making the  $\text{C}_{60}$ -based materials less biocompatible and diminishing its unique properties.<sup>21–30</sup> A new method which can effectively incorporate  $\text{C}_{60}$  into biopolymers such as polysaccharides (e.g., cellulose and/or chitosan) without any reaction is particularly needed. Such a method would make it possible to prepare [CEL/CS+ $\text{C}_{60}$ ] composite material that is not only biocompatible but also has combined unique properties of  $\text{C}_{60}$  and chitosan. This is because chitosan (CS) which is a linear amino polysaccharide, obtained by N-deacetylation of chitin, is the second most abundant naturally

Received: March 7, 2017

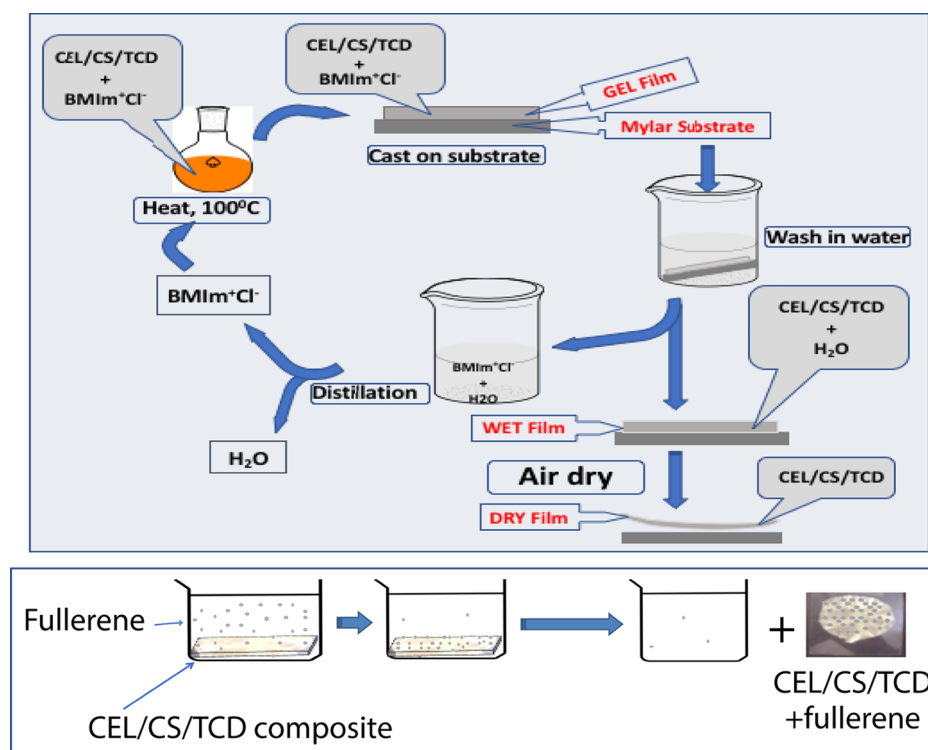
Revised: April 18, 2017

Published: April 25, 2017

Scheme 1. Structures of Compounds Used



Scheme 2



occurring compound. CS is biodegradable, biocompatible, and possesses unique properties including hemostasis, wound healing, bactericide and fungicide, drug delivery, and adsorbent for organic and inorganic pollutants.<sup>31–33</sup>

We have demonstrated recently that a green and simple ionic liquid (IL), butylmethylimidazolium chloride ( $[\text{BMIm}^+\text{Cl}^-]$ ), can dissolve not only CEL and CS but also cyclic oligosaccharides such as  $\alpha$ -,  $\beta$ -, and  $\gamma$ -cyclodextrin ( $\alpha$ -,  $\beta$ -, and  $\gamma$ -CD), and by use of this IL as the sole solvent, we developed a simple, **green**, and totally recyclable method to synthesize

$[\text{CEL}+\text{CS}+\alpha\text{-}/\beta\text{-}/\gamma\text{-CD}]$  composites just by dissolution without using any chemical modifications or reactions.<sup>34</sup> The  $[\text{CEL}+\text{CS}+\alpha\text{-}/\beta\text{-}/\gamma\text{-CD}]$  composites obtained were found to retain unique properties of their components, namely, superior mechanical strength from CEL, hemostasis, heal wounds, kill bacteria, adsorb pollutants from CS, and inclusion complex formation from CD.<sup>34</sup> For example, we found that without CD, CS-based composites can effectively adsorb solute such as polychlorophenols, bisphenol A, in solution, but their adsorption is independent of the size and structure of the analytes.

Conversely, the adsorption by CD-based composites, particularly by  $\gamma$ -CD-based composites exhibits strong dependency on size and structure of the analytes.<sup>34</sup> Clearly, adding  $\gamma$ -CD with its relatively larger cavity into the composite makes it possible to achieve size-selective adsorption through inclusion complex formation with  $\gamma$ -CD. The fact that  $\gamma$ -CD in the [CEL+CS+ $\gamma$ -CD] composite can form an inclusion complex with guest molecules in solution indicates that it may be possible for this composite to form an inclusion complex with C<sub>60</sub> in solution as well. This is because it has been reported that  $\gamma$ -CD with its relatively larger cavity readily forms an inclusion complex with C<sub>60</sub> and its derivatives.<sup>35–37</sup>

The information presented is provocative and clearly indicates that it is possible to develop a method to synthesize novel a C<sub>60</sub>-based composite by a simple adsorption of C<sub>60</sub> derivatives in solution by the [CEL+CS+ $\gamma$ -CD] composite. Such considerations prompted us to initiate this study to investigate the adsorption and desorption of C<sub>60</sub> derivatives by the [CEL+CS+ $\gamma$ -CD] composite and verify that adsorbed C<sub>60</sub> would be retained in the composite to confer the unique properties of C<sub>60</sub> to the composite. Results on adsorption kinetics, adsorption isotherm, desorption, and antimicrobial activity of the composite obtained are reported in this article.

## EXPERIMENTAL SECTION

**Chemicals.** Structures of compounds used in this work are shown in Scheme 1. Microcrystalline cellulose (DP  $\approx$  300) and chitosan (MW 310–375 kDa) were from Sigma-Aldrich and used as received. 1-Methylimidazole and n-chlorobutane (both from Alfa Aesar, Ward Hill, MA) were distilled and subsequently used to synthesize [BMIm<sup>+</sup>Cl<sup>-</sup>] using a method previously reported.<sup>31–33</sup> N-Ethyl-polyamino fullerene (99%) (amino-C<sub>60</sub>) from Bucky USA and polyhydroxy fullerene (99%) (hydroxyl-C<sub>60</sub>) from MER Corporation were used as received. Octakis(2,3,6-tri-O-acetyl)- $\gamma$ -cyclodextrin ( $\gamma$ -TCD) was purchased from Cyclodextrin-Shop, The Netherlands, and used as received. Nutrient broth (NB) and nutrient agar (NA) were obtained from VWR (Radnor, PA). Minimal essential medium (MEM), fetal bovine serum (FBS), and penicillin-streptomycin were obtained from Sigma-Aldrich (St. Louis, MO), whereas Dulbecco's Modified Eagle Medium (DMEM), PBS, and trypsin solution (Gibco) were obtained from Thermo Fischer Scientific (Waltham, MA). CellTiter 96 AQueous One Solution Cell Proliferation Assay was obtained from Promega (Madison, WI). The bacterial cultures and the cell culture of human fibroblasts were purchased from the American Type Culture Collection (ATCC, Rockville, MD).

**Synthesis.** The synthesis of 100%CEL, 100%CS, 50:50 (CEL: $\gamma$ TCD), and 50:50 (CS: $\gamma$ TCD) composites, and full spectroscopic and imaging characterization of the composites, were the same as those used in our earlier studies.<sup>31,33</sup> Essentially, as shown in Scheme 2, an ionic liquid, [BMIm<sup>+</sup>Cl<sup>-</sup>], was used as a solvent to dissolve CEL, CS, and  $\gamma$ -TCD. Dissolution was performed at 100 °C and under Ar or N<sub>2</sub> atmosphere. All polysaccharides were added in portions of approximately 1 wt % of the ionic liquid. Succeeding portions were only added after the previous addition had completely dissolved until the desired concentration has been reached. For composite films, the components were dissolved one after the other, with CEL (or CS) being dissolved first and TCDs last. Using this procedure, solutions of CEL (containing up to 10% w/w (of IL)), CS (up to 4% w/w), and composite solutions containing 50:50 CEL: $\gamma$ -TCD and 50:50 CS: $\gamma$ -TCD were prepared in about 6–8 h.

Upon complete dissolution, the homogeneous solutions of the polysaccharides in [BMIm<sup>+</sup>Cl<sup>-</sup>] were cast onto PTFE molds on glass slides or Mylar sheets to produce thin films. The films were then kept at room temperature for 24 h to allow the solutions to undergo gelation to yield GEL films. Recently, there have been some reports on toxicity of ILs. However, the IL used in this work, [BMIm<sup>+</sup>Cl<sup>-</sup>], is relatively nontoxic compared to other ILs (its EC-50 and LD<sub>50</sub> values

are 897.47 ppm and 550 mg/kg, respectively).<sup>38</sup> Nevertheless, it is desirable to completely remove the IL from regenerated polysaccharide films to ensure the films are biocompatible. Since [BMIm<sup>+</sup>Cl<sup>-</sup>] is totally miscible with water (the logP, its octanol–water partition coefficient, is  $-2.4$ <sup>39</sup>), it was removed from the GEL films by washing the films with water. Washing water (2 L for a composite film of about 10 cm  $\times$  10 cm) was repeatedly replaced with fresh water every 24 h until it was confirmed that IL was not detected in the washed water (by monitoring UV absorption of the IL at 290 nm). It was found that after washing for 72 h, no IL was detected in the washing water by UV measurements. Since the limit of detection of the spectrophotometer used in this work was estimated to be about  $3 \times 10^{-5}$  AU, and the molar absorptivity of [BMIm<sup>+</sup>Cl<sup>-</sup>] at 290 nm is  $2.6 \text{ M}^{-1} \text{ cm}^{-1}$ , it is estimated that if any [BMIm<sup>+</sup>Cl<sup>-</sup>] remains, its concentration would be smaller than  $2 \mu\text{g/mL}$  of the washed water and  $2 \mu\text{g/g}$  of the composite film. Since this concentration is 2 orders of magnitude lower than the LD<sub>50</sub> value of the [BMIm<sup>+</sup>Cl<sup>-</sup>],<sup>38</sup> if any IL remains in the composite films, it would not pose any harmful effect. Furthermore, as we have previously shown that results of UV–vis, FTIR, and NIR techniques confirm that when the composite films were washed with water, [BMIm<sup>+</sup>Cl<sup>-</sup>] was removed from the films to a level not detectable by these techniques.<sup>31–34</sup> Distillation of the washing aqueous solution renders recovery of the [BMIm<sup>+</sup>Cl<sup>-</sup>] for reuse. It was found that at least 88% of [BMIm<sup>+</sup>Cl<sup>-</sup>] was recovered for reuse. Loss of [BMIm<sup>+</sup>Cl<sup>-</sup>] due to its adsorption to the surface of glassware is probably the reason it was not possible to quantitatively recover the IL. The synthesis is, therefore, green and recyclable. Finally, dried composite films were obtained when the wet films were allowed to dry at room temperature in a humidity-controlled chamber.

100%CEL, 100%CS, 50:50 CEL: $\gamma$ -TCD, and 50:50 CS: $\gamma$ -TCD composites containing either hydroxyl-C<sub>60</sub> or amino-C<sub>60</sub> were prepared by first adsorbing the fullerene derivative into corresponding polysaccharide composite following by desorbing any loosely bound fullerene molecules from the composite and finally drying the composite. Adsorption and desorption procedures are described, in details, in the following sections.

**Adsorption of Fullerene Derivatives into Polysaccharide Composites.** The adsorption of the two fullerene derivatives into the 100%CEL, 100%CS, 50:50 CEL: $\gamma$ -TCD, and 50:50 CS: $\gamma$ -TCD composites was monitored by measuring the change in the absorption at 350 nm of solutions of these fullerenes in the presence of the composites. The composite samples (about 0.02 g of dry film of the composite) were washed thoroughly in water prior to the adsorption experiment to ensure they were free of any contamination. To wash the composites, the weighed composite was placed in a thin cell fabricated from PTFE whose windows were covered by two PTFE meshes. The meshes ensured free circulation of water through the material during the washing process. The PTFE mold containing the samples was placed in a 2.0 L beaker which was filled with deionized water and stirred at room temperature for 24 h. The water in the beaker was replaced with fresh deionized water every 4 h.

After 24 h, the composite was taken out of the water and placed into a 1 cm cuvette containing fullerene derivative solution for adsorption studies. During the adsorption process, the solution was stirred using a small magnetic spin bar. In order to prevent damage to the composite sample by the magnetic spin bar and to maximize the circulation of the solution during adsorption, the composite inside the cuvette was sandwiched between two PTFE meshes. Specifically, a piece of PTFE mesh was placed at the bottom of the spectrophotometric cell. The washed polysaccharide composite was laid flat on top of the PTFE mesh. Another piece of PTFE mesh was placed on top of the sample, and finally, the small magnetic spin bar was placed on top of the second mesh. Exactly 2.70 mL of  $1.0 \times 10^{-4}$  M aqueous solution of the fullerene derivative was added to the cuvette. Measurements were carried out on a PerkinElmer Lambda 35 UV/vis spectrometer at 350 nm.

Absorbance of the fullerene in solution was taken at specific time intervals, and the cell was returned to a magnetic stirrer after each measurement for continuous stirring. The concentration of the fullerene derivative in solution decreased in proportion to the amount

of fullerene derivative that was adsorbed by the composite materials. This concentration change was used to calculate the amount of fullerene derivative adsorbed by the composite materials as a function of time.

**Description of Adsorbed Fullerene Derivatives from Composites.** In this measurement, composites were immediately removed from the fullerene derivative solutions after adsorption equilibrium was reached and quickly blotted with dry filter paper to remove any excess solution from the films. The spectrophotometric cells, PTFE meshes, and magnetic spin bar were thoroughly washed and rinsed with deionized water. The composites, which now have fullerene derivative adsorbed on them, were placed back into the clean spectrophotometric cells in an arrangement similar to the one used for the adsorption process. Exactly 2.7 mL of deionized water was pipetted into the cells, and the absorbance of the solution was monitored just like in the adsorption process.

**Procedure Used To Measure Equilibrium Sorption Isotherms.** Batch sorption experiments were carried out in 50 mL stoppered vials containing 10 mL of the fullerene derivative solution of known initial concentration. A weighed amount (0.1 g) of the composite was added to the solution. The samples were agitated at 250 rpm in a shaking water bath at 25 °C for 72 h. The residual amount of fullerene derivative in each flask was determined by its absorbance at 350 nm by UV/vis spectrophotometry. The amount of fullerene derivative adsorbed onto the composite material was calculated using the following mass balance equation:

$$q_e = \frac{(C_i - C_e)V}{m} \quad (1)$$

where  $q_e$  (mg/g) is the equilibrium sorption capacity, and  $C_i$  and  $C_e$  (mg/L) are the initial and final fullerene concentrations, respectively. Also,  $V$  (L) is the volume of the solution, and  $m$  (g) is the weight of the composite material.

**In Vitro Antibacterial Assay.** The composites (100%CEL, 100%CS, CS+ $\gamma$ TCD, CS+ $\gamma$ TCD+hydroxyl- $C_{60}$ , CS+ $\gamma$ TCD+amino- $C_{60}$ ) were tested for potential antibacterial activity against antibiotic-resistant bacteria such as methicillin resistant *S. aureus* (ATCC 33591) (MRSA), *Staphylococcus aureus* (ATCC 25923), *Escherichia coli* (ATCC 8739), and vancomycin resistant *Enterococcus* (ATCC 51299) (VRE), using previously published protocol.<sup>31,32,40</sup> Prior to the assays, cultures were grown overnight at 37 °C with agitation. Composites were cut into 3 mm  $\times$  20 mm stripes and autoclaved at 121 °C and 15 psi for 20 min. The overnight cultures were diluted to 3 mL and put in contact with the material for 24 h. Test tubes with bacteria not exposed to any composite served as a control. The tubes were incubated for 24 h at 37 °C and 600 rpm. After the exposure (time 24 h), the bacteria were diluted and plated onto nutrient agar plates, which were then incubated overnight at 37 °C with agitation. Colony-forming units (CFUs) were counted the next day and compared to the control without composites. The results were expressed as log of reduction in number of bacteria, calculated as  $[\log(N_0/N_{24})]$ , where  $N_0$  is the number of CFUs at the beginning of the experiment, and  $N_{24}$  is the number of bacteria after 24 h). All experiments were carried out in triplicate; the variability between them was expressed as a standard error.

**Biocompatibility Assay.** The biocompatibility of the composites (100%CEL, 100%CS, CS+ $\gamma$ TCD, CS+ $\gamma$ TCD+hydroxyl- $C_{60}$ , CS+ $\gamma$ TCD+amino- $C_{60}$ ) was evaluated with the culture of human fibroblasts (ATCC CRL-2522) through three times as previously published.<sup>31,32,40</sup> The composites in the shape of circles 7 mm in diameter were thermally sterilized by UV light exposure prior to the experiment. Human fibroblasts were grown in a sterile minimal essential medium (MEM) supplemented with 10% FBS and 1% penicillin-streptomycin according to ATCC guidelines and incubated at 37 °C in a humidified atmosphere of 5% CO<sub>2</sub> until the third passage. Cells were seeded in a 24-well plate at a concentration of  $2 \times 10^4$  cells/mL as specified in guidelines for proliferation assay (Promega) and left for 1 day to allow for their attachment. The following day, the sterilized composites were added to the wells and incubated with the

cells for 3 and 7 days. Some wells did not contain composite materials and served as a control. After incubation, the viability and morphology of cells were evaluated with both colorimetric CellTiter 96 AQueous Non-Radioactive Cell Proliferation Assay and an Olympus microscope camera with CellSens imaging software. The procedure for the CellTiter 96 AQueous One Solution Cell Proliferation Assay was followed as specified in the manufacturer's manual. In brief, the MTS reagent was added in a 1:5 ratio to each well after the medium in wells was supplemented with a colorless MEM. The cells were incubated at standard culture conditions for 3 h, and the optical density was measured with a PerkinElmer HTS 7000 Bio Assay Reader at 490 nm. The percent viability was calculated using the following equation:

$$\% \text{ cell viability} = \frac{OD_{\text{Test sample}}}{OD_{\text{Control}}} \times 100 \quad (2)$$

where  $OD_{\text{Test sample}}$  is the measured OD of the test sample well, and  $OD_{\text{Control}}$  is the measured OD of the control well. All experiments were carried out in triplicate; the variability between them was expressed as a standard error.

## RESULTS AND DISCUSSION

The structures of the amino- $C_{60}$  and hydroxyl- $C_{60}$  used in this study are shown in Figure 1. Due to the hydroxyl and amino-

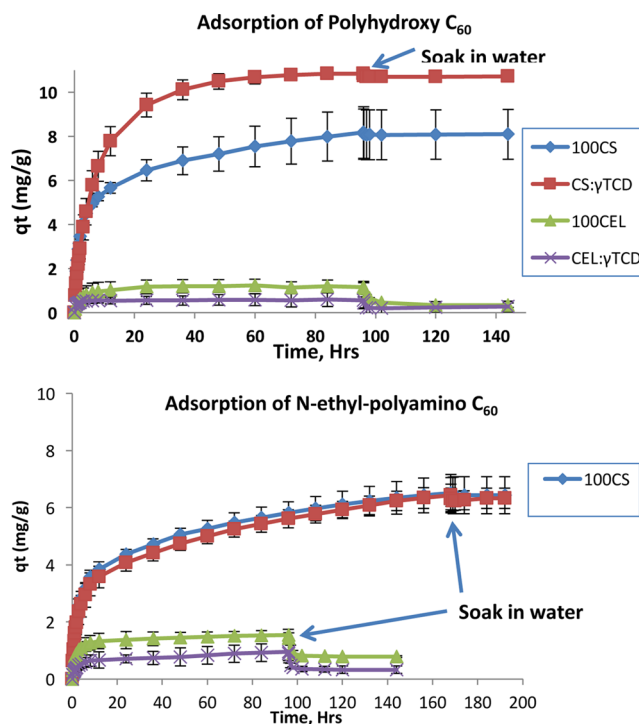


**Figure 1.** Plot of adsorbed amount as a function of time ( $q_t$ ) of polyhydroxy- $C_{60}$  (top) and N-ethyl-polyamino- $C_{60}$  (bottom) by different composites.

ethyl groups, these fullerene compounds are soluble in water. The synthesis and spectroscopic characterization by FTIR, NIR, and XRD of composites containing CEL, CS, and  $\gamma$ -tri-O-acetyl cyclodextrin derivative ( $\gamma$ -TCD) were described in our previous publications.<sup>31–34</sup> As reported previously, these composites have proven to be efficient adsorbents for various organic compounds. As expected, they also exhibit strong adsorption for amino- $C_{60}$  and hydroxyl- $C_{60}$  compounds as well. Plots of adsorbed amounts of fullerene derivatives ( $q_t$ ) as a function of time are shown in Figure 1. As illustrated, CS-based composites (ie., 100%CS and 50:50 CS: $\gamma$ -TCD) have relatively

Table 1. Pseudo-Second-Order Sorption Parameters for Adsorption of Fullerene Derivatives by Different Composites

	pseudo-second-order sorption parameters							
	hydroxy-C <sub>60</sub>				amino-C <sub>60</sub>			
	$q_e$ (mg/g)	$k$ (g/mg Hr <sup>-1</sup> )	$R^2$	MSC	$q_e$ (mg/g)	$k$ (g/mg Hr <sup>-1</sup> )	$R^2$	MSC
100%CS	8 ± 1	0.04 ± 0.02	0.9969	5.6	6.5 ± 0.6	0.022 ± 0.004	0.9942	5.1
50:50CS:γ-TCD	11.58 ± 0.07	0.016 ± 0.003	0.9997	8.1	6.4 ± 0.3	0.019 ± 0.001	0.9914	4.6
100%CEL	1.2 ± 0.3	0.5 ± 0.3	0.9981	6.1	1.6 ± 0.2	0.348 ± 0.005	0.9987	6.7
50:50CEL:γ-TCD	0.6 ± 0.2	0.8 ± 0.3	0.9924	5.0	0.9 ± 0.3	0.3 ± 0.1	0.9882	4.2

Table 2. Adsorption Isotherm Parameters for Adsorption of Amino-C<sub>60</sub> and Hydroxy-C<sub>60</sub> onto 100%CS and [CS+γTCD] Composites

	100%CS									
	Langmuir isotherm parameters			Freundlich isotherm parameters			D-R isotherm parameters			
	$q_{max}$ (mg/g)	$k_L$ (L/mg)	$R^2$	$n$	$k_F$ (mg/g)(L/mg) <sup>1/n</sup>	$R^2$	$q_{max}$ (mg/g)	$\beta$ (mmol <sup>2</sup> J <sup>-2</sup> )	$E$ (kJ/mol)	$R^2$
hydroxy-C <sub>60</sub>	41 ± 3	0.0062	0.9618	2.9	3.26955	0.9926	34.8	0.0035	12.0	0.8074
amino-C <sub>60</sub>	75 ± 5	0.0008	0.9911	1.5	0.34349	0.9852	33.9	0.0130	6.2	0.9212
	[CS+γ-TCD]									
	Langmuir isotherm parameters			Freundlich isotherm parameters			D-R isotherm parameters			
	$q_{max}$ (mg/g)	$k_L$ (L/mg)	$R^2$	$n$	$k_F$ (mg/g)(L/mg) <sup>1/n</sup>	$R^2$	$q_{max}$ (mg/g)	$\beta$ (mmol <sup>2</sup> J <sup>-2</sup> )	$E$ (kJ/mol)	$R^2$
hydroxyl-C <sub>60</sub>	101 ± 29	0.0005	0.9833	1.4	0.22988	0.9891	44.0	0.0429	3.4	0.9661
amino-C <sub>60</sub>	103 ± 18	0.0006	0.9918	1.4	0.28141	0.9901	45.9	0.0281	4.2	0.9598

much higher adsorption capacity for both fullerene compounds than either CEL-based composites. Quantitative assessment of adsorption can be obtained by fitting data to adsorption kinetic models. Data were fitted to pseudo-first-order and pseudo-second-order models. Detailed description of these models, as well as fitted results obtained, are presented in the [Supporting Information \(SI\)](#). On the basis of the  $R^2$  and MSC values, it is clear that the data fit well to the pseudo-second-order model. This is similar as we found in our previous study for the adsorption of other pollutants with these composites. For reference, pseudo-second-order results are listed in [Table 1](#). As listed, the adsorbed amount at equilibrium ( $q_e$ ) of amino-C<sub>60</sub> and hydroxyl-C<sub>60</sub> by 100%CS are 8 ± 1 and 6.5 ± 0.6 mg/g, which are 6 and 4 orders of magnitude higher than the corresponding amounts by 100%CEL of 1.2 ± 0.3 and 1.6 ± 0.2 mg/g. This is hardly surprising as we previously showed that adsorption of various organic compounds as well as of toxins such as microcystin by [CEL+CS] composites is mainly due to the amino groups. As a consequence, CS with its amino groups, not CEL, is responsible for the adsorption of fullerenes. As expected, adding γ-TCD to CS increased the  $q_e$  value for hydroxyl-C<sub>60</sub> from 8 ± 1 to 11.58 ± 0.07 mg/g. However, adsorbed amounts at equilibrium for both hydroxyl-C<sub>60</sub> and amino-C<sub>60</sub> by 100% CEL are, within experimental error, the same as those by 50:50 CEL:γ-TCD. This seems to suggest that adsorption onto CEL and [CEL+γ-TCD] composites is mostly physical sorption onto the surface of the composites. This is also supported by the fact that when the CEL and [CEL+γ-TCD] composites were washed in water most of the adsorbed fullerene molecules rapidly and completely desorbed from these composites.

Results of the kinetic data also seem to indicate that there was no difference in the adsorption of amino-C<sub>60</sub> by 100%CS and [CS+γ-TCD] composites. It is possible that it would take a relatively longer time for amino-C<sub>60</sub> with its bulky N-ethyl amino groups to get included in the cavity of γ-TCD compared to less bulky hydroxyl-C<sub>60</sub>. As a consequence, it is more appropriate to determine adsorption efficiency of the fullerene

compounds not by kinetic data but rather by thermodynamic data. Accordingly, thermodynamic isotherm measurements were carried out for the 100%CS and [CS+γ-TCD] composites as these composites can adsorb a much higher amount of both fullerene derivatives than the corresponding CEL-based composites. The measurement procedure, described in detail in the [Supporting Information](#), is the same as that used in our previous measurements for other organic compounds.<sup>33</sup> Data obtained were fitted to three different models: Langmuir, Freundlich, and Dubinin–Radushkevich, and the results are shown in [Table 2](#). As listed in the table, data fit relatively well to the Langmuir model. According to this model, and as expected, adding γ-TCD to CS increases adsorption of both fullerene compounds. As listed in [Table 2](#) and shown in [Figure 2](#),  $q_{max}$  maximum adsorption capacity value, increases from 41 ± 1 to 101 ± 29 mg/g for hydroxyl-C<sub>60</sub> and from 75 ± 1 to 103 ± 18 mg/g for amino-C<sub>60</sub>. However, while γ-TCD increases adsorption of hydroxyl-C<sub>60</sub> by 146%, it provides only a 37% increase for amino-C<sub>60</sub>. This is probably due to the fact that it is

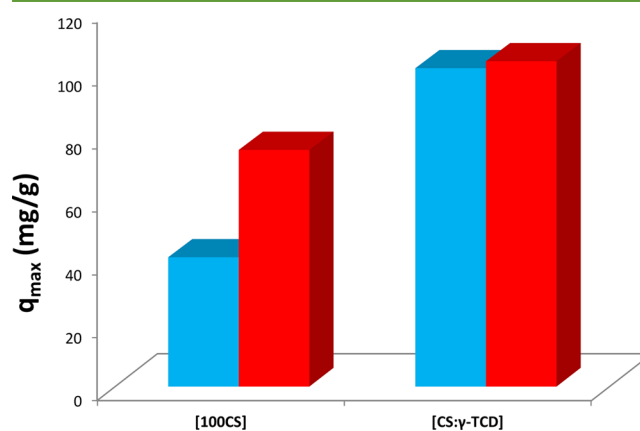
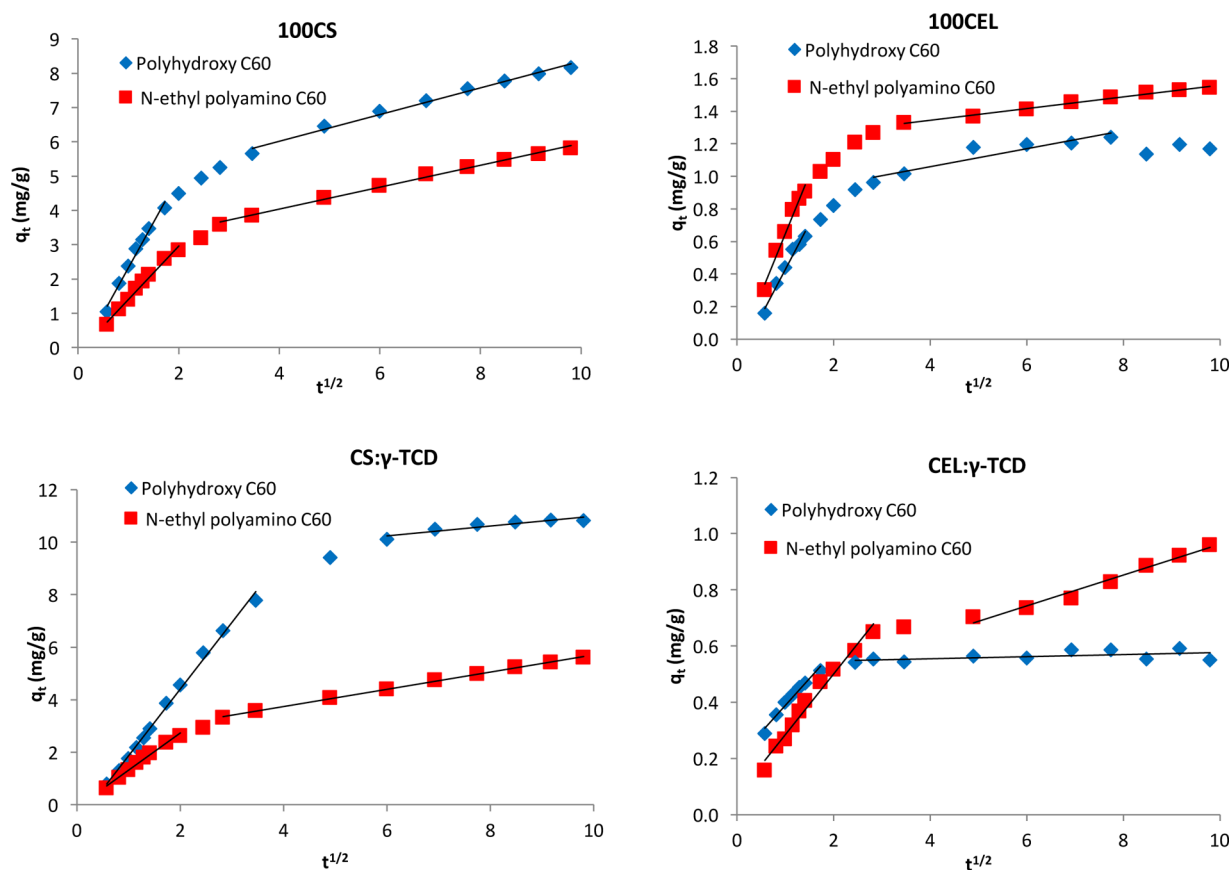


Figure 2. Maximum adsorption capacity ( $q_{max}$ ) of amino-C<sub>60</sub> (red) and hydroxyl-C<sub>60</sub> (blue) by 100%CS and 50:50 CS:γ-TCD composites.



**Figure 3.** Intraparticle diffusion plots of polyhydroxy- $C_{60}$  (blue) and N-ethyl-polyamino- $C_{60}$  (red) by 100%CEL, 100%CS, 50:50 CEL: $\gamma$ -TCD, and 50:50 CS: $\gamma$ -TCD composites.

**Table 3.** Intraparticle Diffusion Rate Constants for Adsorption of Amino- $C_{60}$  and Hydroxy- $C_{60}$  onto 100%CS, 100%CEL, [CS + $\gamma$ TCD], and [CEL+ $\gamma$ -TCD] Composites

	amino- $C_{60}$				hydroxy- $C_{60}$			
	$k_{ip1}$	$R^2$	$k_{ip2}$	$R^2$	$k_{ip1}$	$R^2$	$k_{ip2}$	$R^2$
100%CS	$2.6 \pm 0.1$	0.9857	$0.38 \pm 0.02$	0.9880	$1.55 \pm 0.06$	0.9902	$0.319 \pm 0.009$	0.9950
[CS+ $\gamma$ -TCD]	$2.54 \pm 0.06$	0.9950	$0.18 \pm 0.04$	0.8656	$1.41 \pm 0.06$	0.9888	$0.329 \pm 0.004$	0.9987
100%CEL	$0.56 \pm 0.04$	0.9771	$0.05 \pm 0.01$	0.8806	$0.73 \pm 0.05$	0.9792	$0.036 \pm 0.001$	0.9922
[CEL+ $\gamma$ -TCD]	$0.19 \pm 0.01$	0.9745	$0.004 \pm 0.002$	0.2759	$0.22 \pm 0.01$	0.9766	$0.055 \pm 0.004$	0.9776

relatively more difficult for amino- $C_{60}$  with its bulky N-ethyl amino groups to form inclusion complex with  $\gamma$ -TCD compared to less bulky hydroxyl- $C_{60}$ .

Additional information on the mechanism of the adsorption process can be gained by analyzing kinetic data using the intraparticle diffusion model (detailed description of the model can be found in the [Supporting Information](#)). Figure 3 shows plots of  $q_t$  versus  $t^{1/2}$  for adsorption of amino- $C_{60}$  and hydroxyl- $C_{60}$  by 100%CS, 100%CEL, [CS+ $\gamma$ -TCD], and [CEL+ $\gamma$ -TCD]. It is evident from the plots and from Table 3 that there are two separate stages for all adsorbates and composites. In the first linear portion (Stage I), the adsorbate (amino- $C_{60}$  and hydroxyl- $C_{60}$ ) was rapidly transported from solution through the solution/composite interface and characterized by  $k_{ip1}$ . This can be attributed to the immediate utilization of the most readily available adsorbing sites on surfaces of the composites. The first stage is followed by a much slower Stage II (second linear portion) in which the adsorbate molecules diffuse into the pores within the particle of the composites and consequently are adsorbed by the interior surface of each

particle, which is measured by  $k_{ip2}$ .<sup>33</sup> The diffusion resistance increases and causes a decrease in the diffusion rate. With the continuous uptake of the adsorbate from solution, the adsorption decrease leads to a lower and lower diffusion rate until the final equilibrium is reached. For the 100%CEL and [CEL+ $\gamma$ -TCD] composites, it can be observed that the slope of the second linear region is very small (almost flattening out), which is an indication of very little or no intraparticle diffusion taking place, meaning in these CEL composites adsorption is taking place mostly at the surface, which also explains the low adsorption capacity and the ease with which the adsorbed amino- $C_{60}$  and hydroxyl- $C_{60}$  readily desorb from these CEL composites when they were soaked in water.

Taken together, the results presented above clearly indicate that it is possible to incorporate fullerene derivatives into polysaccharide composites. While the adsorbed fullerene compounds readily, easily, and completely desorb from both CEL and [CEL+ $\gamma$ -TCD] composites, they remain encapsulated in CS and [CS+ $\gamma$ -TCD] composites upon washing in water. This makes it possible, for the first time, to

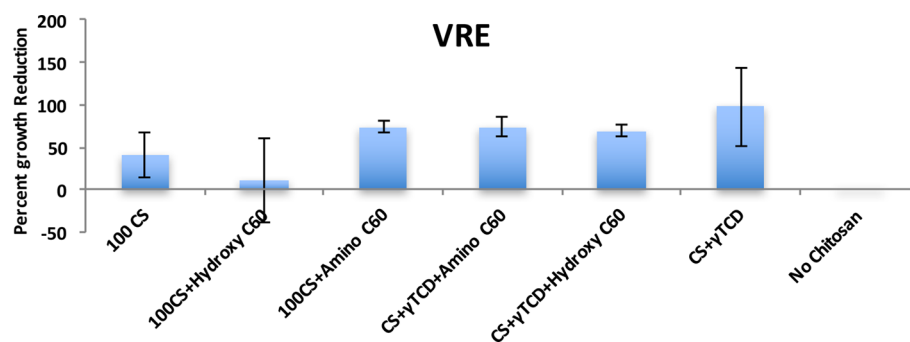


Figure 4. Percent growth reduction of Vancomycin-resistant *Enterococcus* (VRE) after 24 h of exposure to different composites.

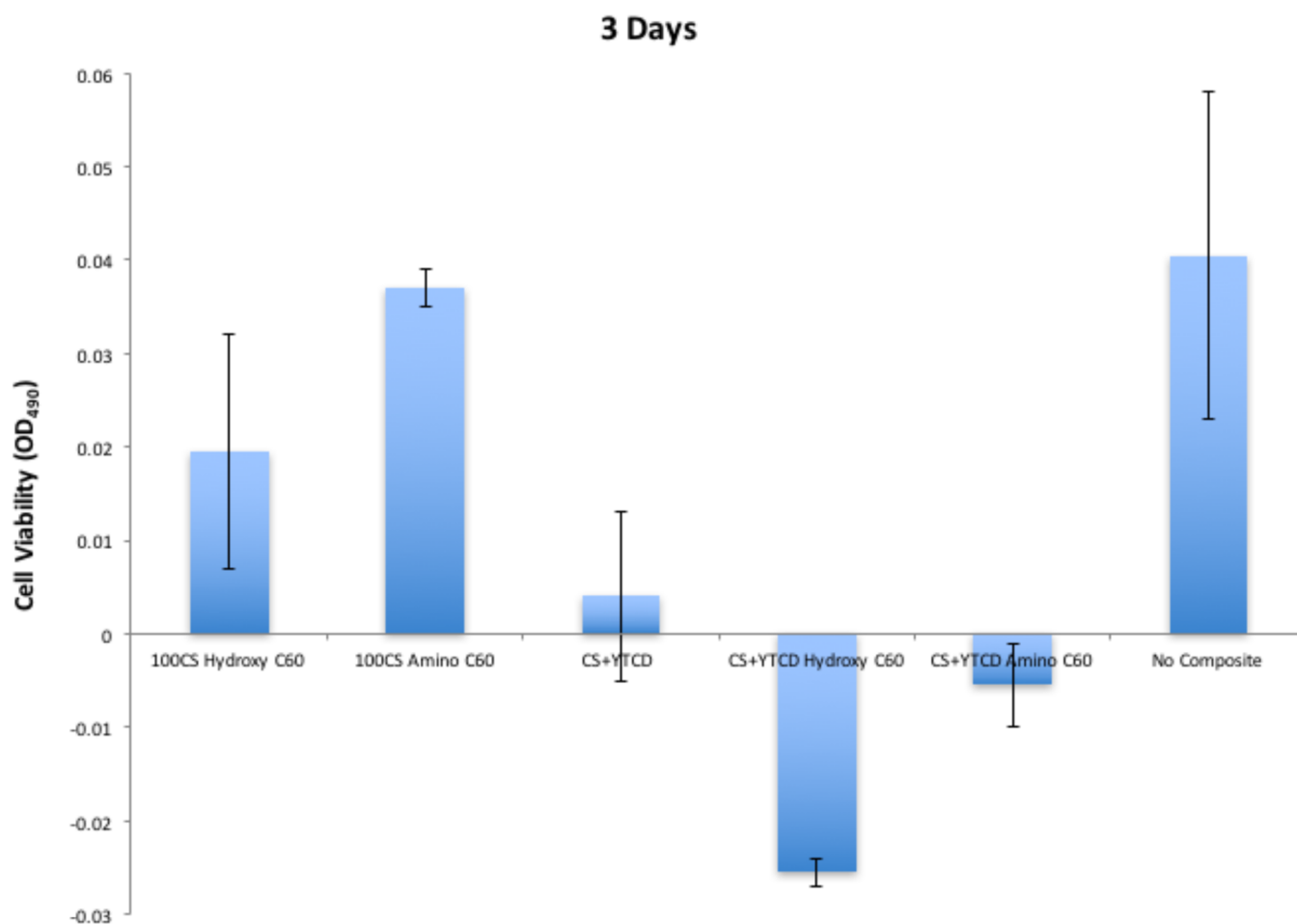


Figure 5. Fibroblast viability based on the absorbance at 490 nm after being exposed to various composites for 3 days.

easily synthesize biocompatible polysaccharide composites containing different fullerene derivatives. It is anticipated that the composites obtained will retain unique properties of its components, including antimicrobial activity by fullerene derivatives. Accordingly, microbial and biocompatibility assays were carried out to determine if the fullerene-based composites synthesized by this method retains the antibacterial property of fullerene and if the CS composites are still biocompatible when fullerene derivatives are incorporated into it.

**Antibacterial Assay.** As described in the [Introduction](#), it has been reported that C<sub>60</sub> exhibits an antibacterial property against some microbial organisms.<sup>7–30</sup> It is not known, however, if fullerene derivatives, particular amino-C<sub>60</sub> and hydroxyl-C<sub>60</sub>, have any bactericidal property when encapsulated

into polysaccharide composites such as CS and CS+γTCD. Accordingly, microbial assays of 100%CS, CS+amino-C<sub>60</sub>, CS+hydroxyl-C<sub>60</sub>, CS+γTCD, CS+γTCD+hydroxyl-C<sub>60</sub>, and CS+γTCD+amino-C<sub>60</sub> composites against various bacteria including *E. coli*, *S. aureus*, VRE, and MRSA. (No assay was carried out for CEL-based composites as we have previously shown that CEL does not possess any antimicrobial activity).<sup>31,32</sup> The bacteria were grown in the presence of the composite and then plated out onto nutrient agar and measured by the number of colonies formed compared to those for the control (no material). Each assay was carried out three times.

The results were calculated as percent growth reduction. It was found that among the four bacteria tested the composites were found to be particularly effective against the antibiotic-

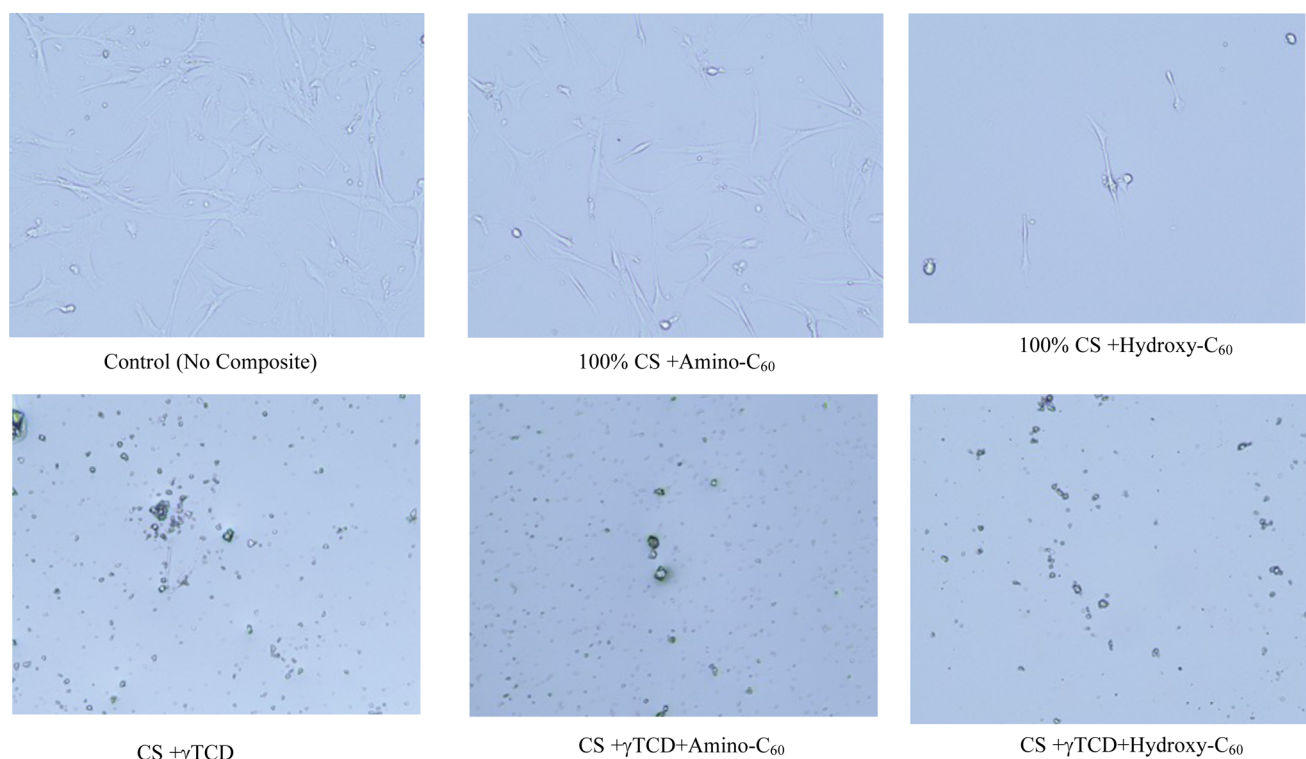


**Figure 6.** Confocal fluorescence images (40X) of human fibroblast in the presence and absence of composites for 3 days. The experiment was performed in duplicate.

resistant bacteria VRE (Figure 4). As expected, on the basis of our previous study,<sup>31,32</sup> 100%CS exhibits antimicrobial activity against VRE. As shown in the figure, adding  $\gamma$ -TCD, amino- $C_{60}$ , and/or hydroxyl- $C_{60}$  to CS substantially increases the percent growth reduction of the composite. For example, adding amino- $C_{60}$  to CS increased the percent growth reduction  $\sim 1.8$  folds (from 40% to 73%) while over a 2.4 times increase in the percent growth reduction was found when  $\gamma$ -TCD was added to CS. It is, therefore, evidently clear that in addition to CS,  $\gamma$ -TCD, amino- $C_{60}$ , and hydroxyl- $C_{60}$  also possess antimicrobial activity against bacteria, particular VRE. In order to use these fullerene-based composites for a bactericide, it is important to determine if the composites are not cytotoxic to human. While CS, being a biopolymer, is biocompatible, it is not known if  $\gamma$ -TCD, amino- $C_{60}$ , and hydroxy- $C_{60}$  are also biocompatible as well. Accordingly, assays were carried out to determine the biocompatibility of the composites.

**Biocompatibility Assay.** To assess a potential cytotoxicity of the CS+amino- $C_{60}$ , CS+hydroxyl- $C_{60}$ , CS+ $\gamma$ TCD, CS + $\gamma$ TCD+hydroxyl- $C_{60}$ , and CS+ $\gamma$ TCD+amino- $C_{60}$  composites, the morphology and the proliferation capabilities of adherent human fibroblasts in the presence and absence of the composites were analyzed. The proliferation capability was assessed using a colorimetric assay CellTiter 96 AQueous Non-Radioactive Cell Proliferation Assay, whereas the morphology of fibroblasts was examined microscopically. Fibroblasts were exposed to composites for 3 days. Viability of fibroblasts in the presence or absence of the composites over time is shown in Figure 5. As illustrated, fibroblast cultures that were treated with [100%CS+amino- $C_{60}$ ] composite had the same metabolic activity as fibroblasts incubated without any composite material. In fact, at 95% confidence interval, fibroblasts exposed to 100CS+hydroxyl- $C_{60}$  and 100%CS+amino- $C_{60}$  composite

showed no statistically significant difference compared to the control (no composite).

Because ISO 10993–5:2009(E) specifies that a material is not cytotoxic if viability of cells after the incubation is above 70%,<sup>41</sup> the results presented clearly indicate that both hydroxyl- $C_{60}$  and amino- $C_{60}$  are not cytotoxic to human when encapsulated into CS composite. Unfortunately, it seems that fibroblast cannot survive after 3 days in the presence of CS + $\gamma$ TCD, CS+ $\gamma$ TCD+hydroxyl- $C_{60}$ , and CS+ $\gamma$ TCD+amino- $C_{60}$ . It seems that  $\gamma$ -TCD, at concentration used in this work (i.e., 50:50 wt/wt CS:  $\gamma$ -TCD) is cytotoxic to human. Since it is known that cytotoxicity is dependent on the concentration of a substance,<sup>40</sup> it is possible that  $\gamma$ -TCD may not be toxic at much lower concentration than the concentration used in this experiment.

Morphological data in Figure 6 shows that the cells that were in contact with 100CS+hydroxyl- $C_{60}$  or 100%CS+amino- $C_{60}$  composite looked relatively healthy. After 3 days, they exhibited an unusual morphology to some extent but were still adherent. There was no difference in viability and morphology of the cells in the presence of these two composites compared to the control (no composite).

## CONCLUSIONS

In summary, we have shown that biocompatible composites containing polysaccharides (CEL, CS, and  $\gamma$ -TCD) and fullerene derivatives (amino- $C_{60}$  and hydroxy- $C_{60}$ ) were successfully synthesized in a green and facile method in which [BMIm<sup>+</sup>Cl<sup>-</sup>], a simple ionic liquid, was used as the sole solvent to prepare 100%CEL, 100%CS, 50:50 CEL: $\gamma$ -TCD, and 50:50 CS: $\gamma$ -TCD composites. The composites were found to readily adsorb amino- $C_{60}$  and hydroxy- $C_{60}$ . Results of adsorption kinetics, adsorption isotherm, and the intraparticle

diffusion model indicate that the fullerene derivatives physically adsorbed onto the surface of the CEL-based composites (i.e., CEL+amino-C<sub>60</sub>, CEL+hydroxy-C<sub>60</sub>, 50:50 CEL:γ-TCD+amino-C<sub>60</sub>, and 50:50 CEL:γ-TCD+hydroxyl-C<sub>60</sub>). As a consequence, the adsorbed fullerene molecules readily and completely desorbed from the CEL-based composites. Conversely, both fullerene derivatives not only strongly adsorbed onto the surface but subsequently diffused into the pores within the matrix of the CS-based composites (i.e., CS+amino-C<sub>60</sub>, CS+hydroxy-C<sub>60</sub>, 50:50 CS:γ-TCD+amino-C<sub>60</sub>, and 50:50 CS:γ-TCD+hydroxyl-C<sub>60</sub>). This made it possible to synthesize the CS+amino-C<sub>60</sub>, CS+hydroxy-C<sub>60</sub>, 50:50 CS:γ-TCD+amino-C<sub>60</sub>, and 50:50 CS:γ-TCD+hydroxyl-C<sub>60</sub> composites. Results of microbial assays show that adding γ-TCD, amino-C<sub>60</sub>, and/or hydroxyl-C<sub>60</sub> to CS substantially increase the ability of the composites to reduce growth of antibiotic-resistant bacteria such as VRE. Results of biocompatibility assays indicate that both hydroxy-C<sub>60</sub> and amino-C<sub>60</sub> are not cytotoxic to human when encapsulated into CS composites. Unfortunately, it seems that human fibroblasts cannot survive after 3 days in the presence of CS+γTCD, CS+γTCD+hydroxyl-C<sub>60</sub>, and CS+γTCD+amino-C<sub>60</sub>. Because hydroxyl-C<sub>60</sub> and amino-C<sub>60</sub> are not cytotoxic and since it is known that cytotoxicity is dependent on concentration, it is possible that lowering the concentration of the γ-TCD may make it possible for all four CS-based composites to be biocompatible and bactericide. Taken together, the results indicate that the (CS+γ-TCD+fullerene) composites with their biocompatibility and bactericide property are particularly suited for use as high performance materials for a wide range of applications including dressing to treat chronic ulcerous infected wounds, nonlinear optics, biosensors, and therapeutic agents. These are the subjects of our current intense investigation.

## ■ ASSOCIATED CONTENT

### Supporting Information

The Supporting Information is available free of charge on the ACS Publication Web site at DOI: The Supporting Information is available free of charge on the [ACS Publications website](https://doi.org/10.1021/acssuschemeng.7b00715) at DOI: [10.1021/acssuschemeng.7b00715](https://doi.org/10.1021/acssuschemeng.7b00715).

Information as mentioned in the text. (PDF)

## ■ AUTHOR INFORMATION

### Corresponding Author

\*Tel. +01 414 288 5428. E-mail: [chieu.tran@marquette.edu](mailto:chieu.tran@marquette.edu).

### ORCID

Chieu D. Tran: [0000-0001-6033-414X](https://orcid.org/0000-0001-6033-414X)

### Notes

The authors declare no competing financial interest.

## ■ REFERENCES

- (1) Kroto, H. W.; Heath, J. R.; O'Brien, S. C.; Curl, R. F.; Smalley, R. E. Buckminsterfullerene. *Nature* **1985**, *318*, 162–163.
- (2) Kratschmer, W.; Fostiropoulos, K.; Huffman, D. R. The infrared and ultraviolet absorption spectra of laboratory-produced carbon dust: evidence for the presence of the C<sub>60</sub> molecule. *Chem. Phys. Lett.* **1990**, *170*, 167.
- (3) Dresselhaus, M. S.; Dresselhaus, G.; Eklund, P. C. *Science of Fullerenes and Carbon Nanotubes*; Academic Press, New York, 1996; pp 1–755.
- (4) Guldi, M. D.; Martín, N. *Fullerenes: From Synthesis to Optoelectronic Properties*; Kluwer Academic Publishers, Dordrecht, The Netherlands, 2002.
- (5) Giacalone, F.; Martín, N. New Concepts and Applications in the Macromolecular Chemistry of Fullerenes. *Adv. Mater.* **2010**, *22*, 4220–4248.
- (6) Milanese, M. E.; Durantini, E. N. Fullerene Derivatives as Antimicrobial Photosensitizing Agents. In *Photodynamic Inactivation of Microbial Pathogens: Medical and Environmental Applications*; Comprehensive Series in Photochemical & Photobiological Sciences, Vol. 11; Royal Society of Chemistry, 2011; pp 161–184.
- (7) Anilkumar, P.; Lu, F.; Cao, L.; Luo, P. G.; Liu, J.-H.; Sahu, S.; Tackett, K. N., II; Wang, Y.; Sun, Y.-P. Fullerenes for applications in biology and medicine. *Curr. Med. Chem.* **2011**, *18*, 2045–2059.
- (8) Chawla, P.; Chawla, V.; Maheshwari, R.; Saraf, S. A.; Saraf, S. K. Fullerenes: from carbon to nanomedicine. *Mini-Rev. Med. Chem.* **2010**, *10*, 662–677.
- (9) Iizumi, Y.; Okazaki, T.; Zhang, M.; Yudasaka, M.; Iijima, S. High efficiencies for singlet oxygen generation of fullerenes and their phototoxicity. *Bull. Chem. Soc. Jpn.* **2008**, *81*, 1584–1588.
- (10) Babavea, E.; Bibli, S.-I.; Tsantili-Kakoulidou, A.; Babavea, E.; Bibli, S.-I.; Tsantili-Kakoulidou, A. Nanomaterials: fullerenes and carbon nanotubes. Structure, physical and chemical properties-biological and therapeutic applications. *Pharmaceutics* **2008**, *2*, 10–21.
- (11) Aroua, S.; Tiu, E. G. V.; Ishikawa, T.; Yamakoshi, Y. Well-Defined Amphiphilic C60-PEG Conjugates: Water-Soluble and Thermoresponsive Materials. *Helv. Chim. Acta* **2016**, *99*, 805–813.
- (12) Bashiri, S.; Vessally, E.; Bekhradnia, A.; Hosseinian, A.; Edjlali, L. Utility of extrinsic [60] fullerenes as work function type sensors for amphetamine drug detection: DFT studies. *Vacuum* **2017**, *136*, 156–162.
- (13) Rather, J. A.; De Wael, K. Fullerene-C60 sensor for ultra-high sensitive detection of bisphenol-A and its treatment by green technology. *Sens. Actuators, B* **2013**, *176*, 110–117.
- (14) Rather, J. A.; De Wael, K. C60-functionalized MWCNT based sensor for sensitive detection of endocrine disruptor vinclozolin in solubilized system and wastewater. *Sens. Actuators, B* **2012**, *171–172*, 907–915.
- (15) Dini, D.; Calvete, M. J. F.; Hanack, M. Nonlinear Optical Materials for the Smart Filtering of Optical Radiation. *Chem. Rev.* **2016**, *116*, 13043–13233.
- (16) Tegos, G. P.; Demidova, T. N.; Arcila-Lopez, D.; Lee, H.; Wharton, T.; Gali, H.; Hamblin, M. R. Cationic fullerenes are effective and selective antimicrobial photosensitizers. *Chem. Biol.* **2005**, *12*, 1127–1135.
- (17) Mashino, T.; Nishikawa, D.; Takahashi, K.; Usui, N.; Yamori, T.; Seki, M.; Endo, T.; Mochizuki, M. Antibacterial and antiproliferative activity of cationic fullerene derivatives. *Bioorg. Med. Chem. Lett.* **2003**, *13*, 4395–4397.
- (18) Aoshima, H.; Kokubo, K.; Shirakawa, S.; Ito, M.; Yamana, S.; Oshima, T. Antimicrobial of fullerenes and their OH derivatives. *Biocontrol Sci.* **2009**, *14*, 69–72.
- (19) Nakamura, S.; Mashino, T. Biological activities of water-soluble fullerene derivatives. *J. Phys.: Conf. Ser.* **2009**, *159*, 159–163.
- (20) Zhang, H. M.; Li, Z.; Uematsu, K.; Kobayashi, T.; Horikoshi, K. Antibacterial activity of cyclodextrins against Bacillus strains. *Arch. Microbiol.* **2008**, *190*, 605–609.
- (21) Stuparu, M. C. Rationally Designed Polymer Hosts of Fullerene. *Angew. Chem., Int. Ed.* **2013**, *52*, 7786–7790.
- (22) Yamakoshi, Y. N.; Yagami, T.; Fukuhara, K.; Sueyoshi, S.; Miyata, N. Solubilization of fullerenes into water with polyvinylpyrrolidone applicable to biological tests. *J. Chem. Soc., Chem. Commun.* **1994**, *4*, 517–518.
- (23) Kawauchi, T.; Kumaki, J.; Kitaura, A.; Okoshi, K.; Kusanagi, H.; Kobayashi, K.; Sugai, T.; Shinohara, H.; Yashima, E. Encapsulation of fullerenes in a helical PMMA cavity leading to a robust processable complex with a macromolecular helicity memory. *Angew. Chem., Int. Ed.* **2008**, *47*, 515–519.
- (24) Moor, K. J.; Osuji, C. O.; Kim, L. H. Dual-functionality fullerene and silver nanoparticle antimicrobial composites via block copolymer templates. *ACS Appl. Mater. Interfaces* **2016**, *8*, 33583–33591.

(25) Alekseeva, O. V.; Sitnikova, O. G.; Bagrovskaya, N. A.; Noskov, A. V. Effect of Polystyrene/Fullerene Composites on the Lipid Peroxidation in Blood Serum. In *Chemical and Structure Modification of Polymers*; Pyrzynski, K., Nyszko, G., Zaikov, G. E., Eds.; Apple Academic Press Inc.: Oakville, Ontario, Canada, 2016; pp 7–8.

(26) Baibarac, M.; Baltog, I.; Daescu, M.; Lefrant, S.; Chirita, P. Optical evidence for chemical interaction of the polyaniline/fullerene composites with N-methyl-2-pyrrolidinone. *J. Mol. Struct.* **2016**, *1125*, 340–349.

(27) Alekseeva, O. V.; Bagrovskaya, N. A.; Noskov, A. V. Physicochemical properties and biological activity of polystyrene/fullerene composites. *Arabian J. Chem.* **2014**, *8* (1–2), 63–94.

(28) Ma, W.; Tumbleston, J. R.; Ye, L.; Wang, C.; Hou, J.; Ade, H. Quantification of nano- and mesoscale phase separation and relation to donor and acceptor quantum efficiency, Jsc, and FF in Polymer: Fullerene Solar Cells. *Adv. Mater.* **2014**, *26*, 4234–4241.

(29) Savagatrup, S.; Makaram, A. S.; Burke, D. J.; Lipomi, D. J. Mechanical properties of conjugated polymers and polymer-fullerene composites as a function of molecular structure. *Adv. Funct. Mater.* **2014**, *24*, 1169–1181.

(30) Zhao, L.; Guo, Z.; Cao, Z.; Zhang, T.; Fang, Z.; Peng, M. Thermal and thermo-oxidative degradation of high density polyethylene/fullerene composites. *Polym. Degrad. Stab.* **2013**, *98*, 1953–1962.

(31) Tran, C. D.; Duri, S.; Harkins, A. L. Recyclable synthesis, characterization, and antimicrobial activity of chitosan-based polysaccharide composite materials. *J. Biomed. Mater. Res., Part A* **2013**, *101A*, 2248–2257.

(32) Harkins, A. L.; Duri, S.; Kloth, L. C.; Tran, C. D. Chitosan-Cellulose Composite for Wound Dressing Material. Part 2. Antimicrobial Activity, Blood Absorption Ability and Biocompatibility. *J. Biomed. Mater. Res., Part B* **2014**, *102*, 1199–1206.

(33) Tran, C. D.; Duri, S.; Delneri, A.; Franko, M. Chitosan-cellulose composite materials: Preparation, Characterization and application for removal of microcystin. *J. Hazard. Mater.* **2013**, *252–253*, 355–366.

(34) Duri, S.; Tran, C. D. Supramolecular composite materials from cellulose, chitosan, and cyclodextrin: facile preparation and their selective inclusion complex formation with endocrine disruptors. *Langmuir* **2013**, *29*, 5037–5049.

(35) Marconi, G.; Mayer, B.; Klein, C. T.; Kohler, G. The structure of higher order C<sub>60</sub>-fullerene- $\gamma$ -cyclodextrin complexes. *Chem. Phys. Lett.* **1996**, *260*, 589–594.

(36) Tseng, W. Y.; Chen, Y. H.; Khairullin, I. I.; Cheng, Y.; Hwang, L. P. NMR study of solid C<sub>60</sub>( $\gamma$ -cyclodextrin). *Solid State Nucl. Magn. Reson.* **1997**, *8*, 219–229.

(37) Seridi, L.; Boufelfel, A. Simulations of docking C<sub>60</sub> in  $\beta$ -cyclodextrin. *J. Mol. Liq.* **2011**, *162*, 69–77.

(38) Docherty, K. M.; Kulpa, C. F., Jr. Toxicity and antimicrobial activity of imidazolium and pyridinium ionic liquids. *Green Chem.* **2005**, *7*, 185–189.

(39) Ropel, L.; Belveze, L. S.; Aki, S. N. V. K.; Stadtherr, M. A.; Brennecke, J. F. Octanol–water partition coefficients of imidazolium-based ionic liquids. *Green Chem.* **2005**, *7*, 83.

(40) Tran, C. D.; Prosenec, F.; Franko, M.; Benzi, G. One-pot synthesis of biocompatible silver nanoparticle composites from cellulose and keratin: Characterization and antimicrobial activity. *ACS Appl. Mater. Interfaces* **2016**, *8*, 34791–34801.

(41) *Biological Evaluation of Medical Devices – Part 5: Tests for in Vitro Cytotoxicity*; ISO 10993; The International Organization for Standardization: Geneva, Switzerland, 2009; [www.iso.org/obp/ui/#iso:std:iso:10993:-5:ed-3:v1:en](http://www.iso.org/obp/ui/#iso:std:iso:10993:-5:ed-3:v1:en) (accessed April 2017).